SIAM J. NUMER. ANAL.
Vol. 45, No. 1, pp. 68–82

FRAMEWORK FOR THE A POSTERIORI ERROR ANALYSIS OF NONCONFORMING FINITE ELEMENTS*

CARSTEN CARSTENSEN†, JUN HU‡, AND ANTONIO ORLANDO§

Abstract. This paper establishes a unified framework for the a posteriori error analysis of a large class of nonconforming finite element methods. The theory assures reliability and efficiency of explicit residual error estimates up to data oscillations under the conditions (H1)–(H2) and applies to several nonconforming finite elements: the Crouzeix–Raviart triangle element, the Han parallelogram element, the nonconforming rotated (NR) parallelogram element of Rannacher and Turek, the constrained NR parallelogram element of Hu and Shi, the P_1 element on parallelograms due to Park and Sheen, and the DSSY parallelogram element. The theory is extended to include 1-irregular meshes with at most one hanging node per edge.

Key words. nonconforming quadrilateral finite elements, a posteriori error analysis

AMS subject classifications. 65N30, 65R20, 73C50

DOI. 10.1137/050628854

1. Introduction.

Nonconforming finite element methods are very appealing for the numerical approximation of partial differential equations, for they enjoy better stability properties compared to the conforming finite elements. While the study of the approximation properties of nonconforming triangular and quadrilateral elements has reached a certain level of maturity [3, 18, 27], the a posteriori error analysis of nonconforming quadrilateral finite element approximations is still in its infancy.

Following the contribution of [16, 15] the a posteriori error analysis for the L^2 norm of the piecewise gradient of the error, $\|\nabla_h e\|_{L^2(\Omega)}$, has been carried out successfully for triangular elements [9, 1] on the basis of two arguments: (a) the Helmholtz decomposition of $\nabla_h e$, and (b) some orthogonality with respect to some conforming finite element space V_h^c. Condition (b) fails for some quadrilateral nonconforming finite elements, e.g., the nonconforming rotated quadrilateral element of Rannacher and Turek, referred to as the NR element [25]. As a result, the a posteriori error analysis of $\|\nabla_h e\|_{L^2(\Omega)}$ for nonconforming quadrilateral elements appears as a minefield. For the NR element, for instance, the work [23] bypasses condition (b) by some enlargement of V_h^{nc} with local bubble trial functions, but their analysis applies only to goal-oriented error control and cannot be extended to the control of $\|\nabla_h e\|_{L^2(\Omega)}$. Another inherent mathematical difficulty for the NR element functions results from the nonequivalence of the continuity at midpoints *and* the equality of integral averages along edges. This makes the operator Π in [2] *not* well defined (while correct for all triangular elements of [1]).

*Received by the editors April 11, 2005; accepted for publication (in revised form) June 30, 2006; published electronically January 12, 2007. This work was supported by the DFG Research Center *MATHEON* “Mathematics for Key Technologies” in Berlin.
http://www.siam.org/journals/sinum/45-1/62885.html

†Institut für Mathematik, Humboldt-Universität zu Berlin, Unter den Linden 6, D-12489 Berlin, Germany (cc@math.hu-berlin.de).

‡LMAM and School of Mathematical Sciences, Peking University, Beijing 100871, People’s Republic of China (hujun@math.pku.edu.cn). The research of this author was supported by the Alexander von Humboldt Foundation through the Alexander von Humboldt Fellowship.

§School of Engineering, Swansea University, Singleton Park, Swansea SA2 8PP, UK (a.orlando@swansea.ac.uk). The research of this author was supported by DFG Schwerpunktprogram 1095.

This paper aims to clarify and develop a unified framework for the a posteriori error analysis of nonconforming finite element methods based on properties for meshes obtained through affine mappings. The resulting framework is exemplified in the two-dimensional elliptic model problem

$$\operatorname{div} \nabla u = f \text{ in } \Omega, \quad u = u_D \text{ on } \Gamma_D, \quad \nabla u \cdot \nu = g \text{ on } \Gamma_N \tag{1.1}$$

on some Lipschitz domain $\Omega \subset \mathbb{R}^2$ with the outward unit normal ν along $\partial\Omega := \Gamma_D \cup \Gamma_N$. Let $V := \{v \in H^1(\Omega) : v = 0 \text{ on } \Gamma_D\}$ denote the space of the test functions approximated by conforming, $V^c_{h,0}$, and nonconforming, $V^{nc}_{h,0}$, finite element spaces associated with a shape regular triangulation $\mathcal{T}$, with $\mathcal{E}$ the set of the edges and $\mathcal{E}(\Omega)$ and $\mathcal{E}(\Gamma_D)$ the interior and boundary edges, respectively. Also, define $[v_h]$ as the jump across $E \in \mathcal{E}(\Omega)$ of the general discontinuous $v_h \in V^{nc}_h$ and $\mathbb{P}_k(\omega)$ the polynomials of total degree k on the domain ω. Throughout the paper, the hypotheses (H1)–(H2) characterize some class of nonconforming finite elements allowing for efficient and reliable error control.

(H1) For all $v_h \in V^{nc}_h$ there holds

$$\int_E [v_h]\, ds = 0 \text{ for } E \in \mathcal{E}(\Omega) \quad \text{and} \quad \int_E (v_h - u_D)\, ds = 0 \text{ for } E \in \mathcal{E}(\Gamma_D). \tag{1.2}$$

(H2) There exists some bounded, linear operator $\Pi : V \mapsto V^{nc}_{h,0}$ and some mesh size independent constant C with the properties (1.3)–(1.5) for every $v_h \in V^c_{h,0}$, $K \in \mathcal{T}$, and $E \in \mathcal{E}$,

$$\int_K \nabla w_h \cdot \nabla (v_h - \Pi v_h)\, dx = 0 \quad \text{for all } w_h \in V^{nc}_h; \tag{1.3}$$

$$\int_K (v_h - \Pi v_h)\, dx = 0; \quad \int_E (v_h - \Pi v_h)\, ds = 0; \tag{1.4}$$

$$\|\nabla\, \Pi v_h\|_{L^2(K)} \le C \|\nabla\, v_h\|_{L^2(K)}. \tag{1.5}$$

The main result of the paper (Theorem 3.1 below) establishes the reliability of

$$\eta^2 := \sum_{K \in \mathcal{T}} \eta_K^2 + \sum_{E \in \mathcal{E}} \eta_E^2, \quad \text{with} \tag{1.6}$$

$$\eta_K^2 := h_K^2 \|f + \operatorname{div} \nabla u_h\|^2_{L^2(K)} \text{ for } K \in \mathcal{T}; \tag{1.7}$$

$$\eta_E^2 := h_E \big(\|J_{E,\nu}\|^2_{L^2(E)} + \|J_{E,\tau}\|^2_{L^2(E)} \big) \text{ for } E \in \mathcal{E}, \tag{1.8}$$

up to the data oscillations $\operatorname{osc}(f)$ and $\operatorname{osc}(g)$ (see section 2.5 below):

$$\|\nabla_h (u - u_h)\|_{L^2(\Omega)} \le C(\eta + \operatorname{osc}(f) + \operatorname{osc}(g)), \tag{1.9}$$

with $J_{E,\nu}$ and $J_{E,\tau}$ defined by (2.9) and (2.10), respectively.

The weak continuity condition (H1) is met by quite a large class of nonconforming finite elements proposed in the literature [14, 19, 25, 17, 24, 21]. However, there are also elements that fail the above condition, for instance, the version of the Rannacher–Turek element [25] with local degree of freedom equal to the value of the function at the midside nodes of each edge, and the nonconforming quadrilateral element of Wilson et al. [29]. Both elements are therefore ruled out by the present analysis.

Condition (H2) represents a key assumption of the theory. It weakens the orthogonality condition (b) mentioned above (see Lemma 3.3 below) by means of an estimate depending on data oscillations and allows the analysis of nonconforming finite elements obtained through affine mappings.

The efficiency of η in the sense that there exists a mesh size–independent constant C such that

$$\eta \leq C(\|\nabla_h e\|_{L^2(\Omega)} + \mathrm{osc}(f) + \mathrm{osc}(u_D) + \mathrm{osc}(g)), \tag{1.10}$$

with $\mathrm{osc}(u_D)$ defined in section 2.5, can be proved by adapting the arguments from [28, pp. 15–18] and [16, 9].

An outline of the remaining parts of the paper is as follows. Section 2 displays the setup of the model problem (1.1), and introduces the conforming and nonconforming finite element spaces as well as the a posteriori error estimate (1.6) and the data oscillations in (1.9). Theorem 3.1 shows that the abstract conditions (H1)–(H2) imply the reliability in the sense of (1.9). This is stated and proved in section 3 in the abstract framework, while the relevant examples follow in section 4. Namely, applications of the theory are given for the Crouzeix–Raviart element, the Han element [19], the NR element [25] with local degrees of freedom equal to the average value over the edges, the constrained NR element of Hu and Shi [21], the P_1 quadrilateral element of Park and Sheen [24], and the DSSY element [17]. Section 4 concludes with a discussion of the applicability of the theory to 1-irregular meshes, with at most one hanging node per edge, and its generalization to elliptic systems. Section 5 describes an adaptive finite element method and a numerical example for the NR element with hanging nodes.

2. Notation and preliminaries.

2.1. Model problem. Let Ω be a polygonal domain in $\mathbb{R}^2$ with boundary $\Gamma := \partial\Omega$ split into a closed Dirichlet boundary $\Gamma_D \subseteq \Gamma$ with positive surface measure and the remaining Neumann boundary $\Gamma_N := \Gamma \setminus \Gamma_D$. Given $f \in L^2(\Omega)$, $g \in L^2(\Gamma_N)$, $u_D \in H^{1/2}(\Gamma_D)$, and $V := \{v \in H^1(\Omega) : v = 0 \text{ on } \Gamma_D\}$, the solution of (1.1) satisfies

$$\int_\Omega \nabla u \cdot \nabla v \, dx = \int_\Omega f v \, dx + \int_{\Gamma_N} g v \, ds \quad \text{for every } v \in V, \tag{2.1}$$

where the symbol $\cdot$ is the scalar product in the Euclidean space $\mathbb{R}^2$. Furthermore, we denote by L^2 the Lebesgue space of square integrable functions, and by H^s with $s > 0$ the Sobolev space defined in the usual way [18]. For the corresponding norm we use the symbols $\|\cdot\|_{L^2}$ and $\|\cdot\|_{H^s}$, respectively, with explicit indication of the domain of integration. With Ω an open set of $\mathbb{R}^2$, and $\varphi \in H^1(\Omega)$, the curl and gradient operators are given as

$$\mathrm{curl}\,\varphi = (-\partial\varphi/\partial x_2,\, \partial\varphi/\partial x_1), \quad \nabla\varphi = (\partial\varphi/\partial x_1,\, \partial\varphi/\partial x_2), \tag{2.2}$$

whereas for an $\mathbb{R}^2$-valued function $v = (v_1, v_2)$ the divergence is

$$\mathrm{div}\, v = \partial v_1/\partial x_1 + \partial v_2/\partial x_2. \tag{2.3}$$

Throughout the paper, the letter C denotes a generic constant, not necessarily the same at each occurrence.

2.2. Conforming finite element spaces. For approximating (2.1) by the finite element method, we introduce a regular triangulation $\mathcal{T}$ of $\bar{\Omega} \subset \mathbb{R}^2$ in the sense of Ciarlet [12, 6] into closed triangles, and/or convex quadrilaterals, such that $\bigcup_{K \in \mathcal{T}} K = \bar{\Omega}$, two distinct elements K and K' in $\mathcal{T}$ are either disjoint, or share the common edge E, or a common vertex; that is, hanging nodes at this stage are not allowed, and we refer to section 4.6 and [11] for further discussion. Let $\mathcal{E}$ denote the set of all edges in $\mathcal{T}$, $\mathcal{N}$ the set of vertices of the elements $K \in \mathcal{T}$, and $\mathcal{N}_m$ the set of the midside nodes m_E of the edges $E \in \mathcal{E}$. The set of interior edges of Ω are denoted by $\mathcal{E}(\Omega)$, the set of edges of the element K by $\mathcal{E}(K)$, whereas those that belong to the Dirichlet and Neumann boundary are denoted by $\mathcal{E}(\Gamma_D)$ and $\mathcal{E}(\Gamma_N)$, respectively. For the set of midpoints of the edges $E \in \mathcal{E}(\Gamma_D)$ we use the notation $\mathcal{N}_m(\Gamma_D)$. By h_K and h_E we denote the diameter of the element $K \in \mathcal{T}$ and of the edge $E \in \mathcal{E}$, respectively. Also, we denote by ω_K the patch of elements $K' \in \mathcal{T}$ that share an edge with K, and by ω_E the patch of elements having in common the edge E. Given any edge $E \in \mathcal{E}$ we assign one fixed unit normal ν_E; if (ν_1, ν_2) are its components, τ_E denotes the orthogonal vector of components $(-\nu_2, \nu_1)$. For $E \in \mathcal{E}(\Gamma_D) \cup \mathcal{E}(\Gamma_N)$ on the boundary we choose $\nu_E = \nu$, the unit outward normal to Ω, and concordantly the unit tangent vector τ. Once ν_E and τ_E have been fixed on E, in relation to ν_E one defines the elements $K_{in} \in \mathcal{T}$ and $K_{out} \in \mathcal{T}$, with $E = K_{out} \cap K_{in}$, as depicted in Figure 1.

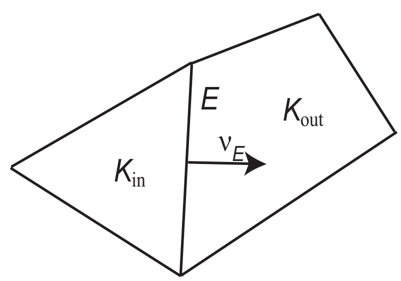

FIG. 1. *Definition of the elements K_{in} and K_{out} in relation to ν_E.*

Given $E \in \mathcal{E}(\Omega)$ and an $\mathbb{R}^d$-valued function v defined in Ω, with $d = 1, 2$, we denote by $[v]_E$ the jump of v across E, that is,

$$[v]_E(x) = (v|_{K_{out}}(x) - v|_{K_{in}}(x)) \quad \text{for } x \in E = K_{in} \cap K_{out};$$

the subscript E will be omitted whenever it is clear from the context.

With the triangulation $\mathcal{T}$ we associate, moreover, the space $H^1(\mathcal{T})$ defined as

$$H^1(\mathcal{T}) = \{v \in L^2(\Omega) : \forall K \in \mathcal{T},\, v|_K \in H^1(K)\},$$

and for $v \in H^1(\mathcal{T})$, we denote by $\nabla_h v$ the gradient operator defined piecewise with respect to $\mathcal{T}$, i.e.,

$$\nabla_h v|_K := \nabla(v|_K).$$

Whenever it is clear from the context that we are considering the restriction of v to an element $K \in \mathcal{T}$, then we clearly write only ∇v in lieu of $\nabla_h v$.

For a nonnegative integer k the space $Q_k(\omega)$ consists of polynomials of total degree at most k defined over ω in the case in which $\omega = K$ is a triangle, whereas it denotes polynomials of degree at most k in each variable in the case in which K is a quadrilateral. For this presentation it will suffice to assume $k = 1$. The corresponding conforming space will be denoted by

$$V_h^c := \{v \in H^1(\Omega) : v|_K \in Q_1(K)\} \quad \text{and} \quad V_{h,0}^c := \{v \in V_h^c : v = 0 \text{ on } \Gamma_D\}.$$

Throughout the paper, for triangular elements, $V_{h,0}^c$ stands for the conforming space of P_1 elements, whereas for quadrilateral elements it denotes the conforming space of bilinear elements.

Given the conforming finite element space $V_{h,0}^c$, we consider the Clément interpolation operator or any other regularized conforming finite element approximation operator $\mathcal{J} : H^1(\Omega) \mapsto V_h^c$ with the property

$$\|\nabla \mathcal{J}\varphi\|_{L^2(K)} + \|h_K^{-1}(\varphi - \mathcal{J}\varphi)\|_{L^2(K)} \leq C\|\nabla\varphi\|_{L^2(\omega_K)}, \tag{2.4}$$

$$\|h_E^{-1/2}(\varphi - \mathcal{J}\varphi)\|_{L^2(E)} \leq C\|\nabla\varphi\|_{L^2(\omega_E)} \tag{2.5}$$

for all $K \in \mathcal{T}$, $E \in \mathcal{E}$, and $\varphi \in H^1(\Omega)$. The existence of such operators is guaranteed, for instance, in [13, 26, 7, 5].

2.3. Nonconforming finite element spaces and a posteriori error estimator. A nonconforming finite element approximation is defined by a finite-dimensional trial space $V_h^{nc} \subset H^1(\mathcal{T})$ along with the test space $V_{h,0}^{nc}$ corresponding to the discrete homogeneous Dirichlet boundary conditions. The nonconforming finite element approximation $u_h \in V_h^{nc}$ of (2.1) then satisfies

$$\int_\Omega \nabla_h u_h \cdot \nabla_h v_h \, dx = \int_\Omega f v_h \, dx + \int_{\Gamma_N} g v_h \, ds \quad \text{for every } v_h \in V_{h,0}^{nc}. \tag{2.6}$$

The Helmholtz decomposition is a well-established tool in the a posteriori error analysis of nonconforming finite element methods [16, 9].

LEMMA 2.1. *Given any $e \in V + V_h^{nc}$ such that $\nabla_h e \in L^2(\Omega; \mathbb{R}^2)$ there exist $w, \varphi \in H^1(\Omega)$ with $w = 0$ on Γ_D, and $\nabla\varphi \cdot \tau = \operatorname{curl}\varphi \cdot \nu = 0$ on Γ_N such that*

$$\nabla_h e = \nabla w + \operatorname{curl}\varphi, \tag{2.7}$$

$$\|\nabla_h e\|_{L^2(\Omega)}^2 = \|\nabla w\|_{L^2(\Omega)}^2 + \|\operatorname{curl}\varphi\|_{L^2(\Omega)}^2. \tag{2.8}$$

2.4. A posteriori error estimator. For each edge $E \in \mathcal{E}$, define $J_{E,\nu}$ the jump of $\nabla_h u_h$ across E in direction ν_E, i.e.,

$$J_{E,\nu} := \begin{cases} [\nabla_h u_h]_E \cdot \nu_E & \text{if } E \in \mathcal{E}_\Omega, \\ g - \nabla u_h \cdot \nu & \text{if } E \in \mathcal{E}_N, \\ 0 & \text{if } E \in \mathcal{E}_D, \end{cases} \tag{2.9}$$

and $J_{E,\tau}$ the jump of $\nabla_h u_h$ across E in direction t_E, i.e.,

$$J_{E,\tau} := \begin{cases} [\nabla_h u_h]_E \cdot \tau_E & \text{if } E \in \mathcal{E}_\Omega, \\ 0 & \text{if } E \in \mathcal{E}_N, \\ (\nabla u_D - \nabla u_h) \cdot \tau & \text{if } E \in \mathcal{E}_D, \end{cases} \tag{2.10}$$

and recall η from (1.6) with the local contributions η_K (1.7) and η_E (1.8) for each $K \in \mathcal{T}$ and $E \in \mathcal{E}$, respectively.

2.5. Data oscillations. For $f \in L^2(\Omega)$ and its piecewise constant approximation f_h with respect to $\mathcal{T}$, we refer to $\operatorname{osc}(f)$ as the oscillation of f [28],

$$\operatorname{osc}^2(f) := \sum_{K\in\mathcal{T}} h_K^2 \|f - f_h\|^2_{L^2(K)}, \tag{2.11}$$

with $\operatorname{osc}(f)$ being a higher order term if $f \in H^1(\Omega)$. Similar definitions hold for the oscillations $\operatorname{osc}(u_D)$ and $\operatorname{osc}(g)$ of the Dirichlet and Neumann boundary data, $u_D \in H^{1/2}(\Gamma_D)$ and $g \in L^2(\Gamma_N)$, and their piecewise affine and constant approximations $u_{D,h}$ and g_h, respectively, as [28, 8]

$$\operatorname{osc}^2(u_D) := \sum_{E\in\mathcal{E}(\Gamma_D)} h_E \left\| \frac{\partial}{\partial s}(u_D - u_{D,h}) \right\|^2_{L^2(E)},$$

$$\operatorname{osc}^2(g) := \sum_{E\in\mathcal{E}(\Gamma_N)} h_E \|g - g_h\|^2_{L^2(E)}.$$

3. Reliability of $\boldsymbol{\eta}$. This section presents the main result of this paper, that is, (H1)–(H2) imply the reliability of η. Throughout this section, let u solve (2.1), let u_h solve (2.6), and set $e := u - u_h$.

THEOREM 3.1. *Assume that the space V_h^{nc} along with the corresponding $V_{h,0}^{nc}$ satisfy* (H1)–(H2). *Then there exists a positive constant C depending only on the minimum angle of $\mathcal{T}$ such that η is reliable in the sense that*

$$\|\nabla_h e\|_{L^2(\Omega)} \le C\big(\eta + \operatorname{osc}(f) + \operatorname{osc}(g)\big). \tag{3.1}$$

The remainder of this section is devoted to the proof of Theorem 3.1.

We establish first some interpolation error estimates for the operator Π in (H2).

LEMMA 3.2. *Given the operator Π meeting* (H2)*, there then exists some mesh size–independent constant C such that there holds*

$$\begin{aligned} h_K^{-1}\|v_h - \Pi v_h\|_{L^2(K)} + \|\nabla(v_h - \Pi v_h)\|_{L^2(K)} &\le C\|\nabla v_h\|_{L^2(K)}, \\ h_E^{-1/2}\|v_h - \Pi v_h\|_{L^2(E)} &\le C\|\nabla v_h\|_{L^2(\omega_E)}. \end{aligned} \tag{3.2}$$

Proof. Let Π_0^K denote the mean average operator over K. Using condition $(1.4)_1$ with $\Pi_0^K v_h = \Pi_0^K\,\Pi\, v_h$, the triangular inequality, and (1.5), one obtains

$$\begin{aligned} \|v_h - \Pi v_h\|_{L^2(K)} &\le \|v_h - \Pi_0^K v_h\|_{L^2(K)} + \|\Pi_0^K \Pi v_h - \Pi v_h\|_{L^2(K)} \\ &\le C(h_K\|\nabla v_h\|_{L^2(K)} + h_K\|\nabla v_h\|_{L^2(K)}). \end{aligned} \tag{3.3}$$

A triangular inequality and (1.5) also gives

$$\|\nabla v_h - \nabla\,\Pi v_h\|_{L^2(K)} \le C\|\nabla v_h\|_{L^2(K)},$$

which, combined with (3.3), finally yields $(3.2)_1$. Arguing in a similar way and using the trace theorem [6, 12] one obtains $(3.2)_2$. ∎

Here and throughout, f_h and g_h denote piecewise constant approximations of f and g, respectively. From (H2) and for every $v_h \in V_{h,0}^c$, the following holds:

$$\int_\Omega \nabla_h u_h \cdot \nabla v_h\,dx = \int_\Omega f\,\Pi v_h\,dx + \int_{\Gamma_N} g\,\Pi v_h\,ds. \tag{3.4}$$

LEMMA 3.3. *There exists a mesh size–independent constant C such that, for every $v_h \in V^c_{h,0}$, the following holds:*

$$\int_\Omega \nabla_h e \cdot \nabla v_h \, dx \leq C(\operatorname{osc}(f) + \operatorname{osc}(g)) \, \|\nabla v_h\|_{L^2(\Omega)}. \tag{3.5}$$

Proof. From (2.1) and (3.4), for every $v_h \in V^c_{h,0}$ it follows that

$$\int_\Omega \nabla_h e \cdot \nabla v_h \, dx = \sum_{K \in \mathcal{T}} \left(\int_K (f - f_h)(v_h - \Pi v_h) \, dx + \int_K f_h (v_h - \Pi v_h) \, dx \right) + \sum_{E \in \mathcal{E}(\Gamma_N)} \left(\int_E (g - g_h)(v_h - \Pi v_h) \, ds + \int_E g_h (v_h - \Pi v_h) \, ds \right).$$

Since (1.4), this equals

$$\int_\Omega (f - f_h)(v_h - \Pi v_h) \, dx + \int_{\Gamma_N} (g - g_h)(v_h - \Pi v_h) \, ds.$$

The combination of Cauchy inequalities with (3.2) yields its upper bound:

$$C\Bigg(\Big(\sum_{K \in \mathcal{T}} h_K^2 \|f - f_h\|^2_{L^2(K)} \Big)^{1/2} + \Big(\sum_{E \in \mathcal{E}(\Gamma_N)} h_E \|g - g_h\|^2_{L^2(E)} \Big)^{1/2} \Bigg) \|\nabla v_h\|_{L^2(\Omega)}. \qquad \square$$

Remark 1. If $V^c_{h,0}$ is a subspace of $V^{nc}_{h,0}$, then (H1)–(H2) hold for $\Pi = I$ and (3.5) recovers the L^2-orthogonality of $\nabla_h e$ and ∇v_h for every $v_h \in V^c_{h,0}$ (because $C = 0$ in (3.2)).

The following orthogonality condition (3.6) is well established in the literature on a posteriori error estimates for nonconforming finite element schemes.

LEMMA 3.4. *For every $v_h \in V^c_h$ such that $\partial v_h / \partial s = 0$ on Γ_N, it holds that*

$$\int_\Omega \nabla_h e \cdot \operatorname{curl} v_h \, dx = 0. \tag{3.6}$$

Proof. The proof is along the lines of [16, eqn. (3.4)] for the Crouzeix–Raviart element. An integration by parts over each element gives

$$\int_\Omega \nabla_h e \cdot \operatorname{curl} v_h \, dx = \sum_{E \in \mathcal{E}} \int_E [u - u_h] \frac{\partial v_h}{\partial s} \, ds. \tag{3.7}$$

Since for $v_h \in V^c_h$, $\partial v_h / \partial s$ is constant over each edge $E \in \mathcal{E}(\Omega) \cup \mathcal{E}(\Gamma_D)$, or is zero on $E \in \mathcal{E}(\Gamma_N)$, accounting for (H1), one obtains (3.6). $\square$

The proof of (3.1) starts with the decomposition (2.7), the interpolation operator $\mathcal{J}$ of Clément, and Lemma 3.4. Without loss of generality one can choose φ in (2.7) to be equal to a constant on Γ_N, and $\mathcal{J}\varphi|_{\Gamma_N} = \varphi|_{\Gamma_N}$. Then it follows that

$$\|\nabla_h e\|^2_{L^2(\Omega)} = \int_\Omega \nabla_h e \cdot (\nabla w + \operatorname{curl} \varphi) \, dx = \int_\Omega \nabla_h e \cdot \nabla (w - \mathcal{J} w) \, dx + \int_\Omega \nabla_h e \cdot \operatorname{curl}(\varphi - \mathcal{J}\varphi) \, dx + \int_\Omega \nabla_h e \cdot \nabla \mathcal{J} w \, dx.$$

From Lemma 3.3 and the estimate (2.4), one obtains

$$
\begin{aligned}
\int_\Omega \nabla_h e \cdot \nabla \mathcal{J} w \, dx &\le C\big(\operatorname{osc}(f) + \operatorname{osc}(g)\big) \|\nabla \mathcal{J} w\|_{L^2(\Omega)} \\
&\le C\big(\operatorname{osc}(f) + \operatorname{osc}(g)\big) \|\nabla w\|_{L^2(\Omega)}.
\end{aligned} \tag{3.8}
$$

Since $(w - \mathcal{J}w)$ and $(\varphi - \mathcal{J}\varphi)$ belong to $H^1(\Omega)$, the use of the Stokes theorem and Green's formula over each element gives, after some rearrangements,

$$
\begin{aligned}
&\int_\Omega \nabla_h e \cdot \nabla(w - \mathcal{J}w)\, dx + \int_\Omega \nabla_h e \cdot \operatorname{curl}(\varphi - \mathcal{J}\varphi)\, dx \\
&= \sum_{E \in \mathcal{E}} \left(\int_E J_{E,\tau} (\varphi - \mathcal{J}\varphi)\, ds + \int_E J_{E,\nu} (w - \mathcal{J}w)\, ds \right) \\
&+ \sum_{K \in \mathcal{T}} \int_K (f + \operatorname{div} \nabla u_h)\,(w - \mathcal{J}w)\, dx.
\end{aligned}
$$

It is a standard argument with Cauchy inequalities and (2.4)–(2.5) to bound this by

$$
C\eta\big(\|\nabla w\|_{L^2(\Omega)} + \|\nabla \varphi\|_{L^2(\Omega)}\big),
$$

with η from (1.6). The combination of the aforementioned estimates with (2.8) concludes the proof of (3.1).

4. Examples. In this section, we verify (H1)–(H2) for several nonconforming finite elements proposed in the literature and discuss the applicability of the theory to 1-irregular meshes and to elliptic systems in divergence form. For the following examples, the operator Π that enters (H2) is the interpolation operator of V associated with $V_{h,0}^{nc}$.

4.1. The Crouzeix–Raviart element. The nonconforming finite element space associated with the Crouzeix–Raviart element [14] reads

$$
\begin{aligned}
V_h^{nc} := \big\{ v_h \in H^1(\mathcal{T}) : v_h|_K \in P_1(K) \quad \forall K \in \mathcal{T},\ v_h \text{ is continuous at each} \\
m_E \in \mathcal{N}_m \setminus \mathcal{N}_m(\Gamma_D), \text{ and } v_h(m_E) = u_D(m_E) \text{ for } m_E \in \mathcal{N}_m(\Gamma_D) \big\},
\end{aligned} \tag{4.1}
$$

and $V_{h,0}^{nc}$ denotes the space corresponding to the discrete homogeneous Dirichlet boundary conditions. For this element, it is trivial to check that the space V_h^{nc} meets (H1). Furthermore, since $V_{h,0}^{c} \subset V_{h,0}^{nc}$, (H2) follows immediately (see Remark 1) and Theorem 3.1 recovers the results of [16, 9].

4.2. The Han element. With respect to the global coordinate system (x_1, x_2), the nonparametric formulation of rectangular and parallelogram elements proposed by Han in [19] is obtained by introducing the local space

$$
\mathcal{Q}_{\mathcal{H}}^{nc} = \operatorname{span}\left\{ 1,\, x_1,\, x_2,\, x_1^2 - \frac{5}{3}x_1^4,\, x_2^2 - \frac{5}{3}x_2^4 \right\}, \tag{4.2}
$$

and the $\mathcal{Q}_{\mathcal{H}}^{nc}$-unisolvent set of linearly independent linear forms [12, 19] reads

$$
\mathcal{F}_E(v) = \frac{1}{h_E} \int_E v\, ds, \quad \mathcal{F}_K(v) = \frac{1}{|K|} \int_K v\, dx \text{ with } E \in \mathcal{E}(K), \quad K \in \mathcal{T}. \tag{4.3}
$$

This defines the five degrees of freedom for the Han element. In (4.3), $|K|$ denotes the area of the element. Recall from [12] that, given $E = K \cap K'$ for K, $K' \in \mathcal{T}$, and $v \in H^1(\mathcal{T})$ such that $v|_K \in \mathcal{Q}_{\mathcal{H}}^{nc}(K)$ and $v|_{K'} \in \mathcal{Q}_{\mathcal{H}}^{nc}(K')$, we say that v is continuous with respect to $\mathcal{F}_E$ if $\mathcal{F}_E(v|_K) = \mathcal{F}_E(v|_{K'})$. The nonconforming finite element space V_h^{nc} is then defined as

$$\begin{aligned} V_h^{nc} := \big\{ v \in H^1(\mathcal{T}) : v|_K \in \mathcal{Q}_{\mathcal{H}}^{nc}(K) \text{ for each } K \in \mathcal{T},\ v \text{ continuous with respect} \\ \text{to } \mathcal{F}_E\ \forall\ E \in \mathcal{E}(\Omega), \text{ and } \mathcal{F}_E(v) = \mathcal{F}_E(u_D)\ \forall\ E \in \mathcal{E}(\Gamma_D) \big\}, \end{aligned} \tag{4.4}$$

whereas $V_{h,0}^{nc}$ denotes the space corresponding to the discrete homogeneous Dirichlet boundary conditions in (4.4). For $v_h \in V_h^{nc}$, the definition (4.4) of V_h^{nc} and (4.3) yield

$$\int_E [v_h]\, ds = 0 \ \text{ for all } E \in \mathcal{E}(\Omega) \quad \text{ and } \quad \int_E (v_h - u_D)\, ds = 0 \ \text{ for all } E \in \mathcal{E}(\Gamma_D), \tag{4.5}$$

and so V_h^{nc} verifies (H1). Let V_h^c be the conforming space of the bilinear elements constructed from the local spaces $\mathcal{Q}^c(K) = \operatorname{span}\{1, x_1, x_2, x_1x_2\}$. Consider then the interpolation operator $\Pi : V \mapsto V_{h,0}^{nc}$ defined by the following conditions: For all $E \in \mathcal{E}(K)$ and $K \in \mathcal{T}$,

$$\Pi v \in V_{h,0}^{nc}, \quad \mathcal{F}_E(\Pi v|_K) = \mathcal{F}_E(v|_K), \quad \mathcal{F}_K(\Pi v|_K) = \mathcal{F}_K(v|_K). \tag{4.6}$$

Given $v \in V_{h,0}^c$, the restriction of v to $K \in \mathcal{T}$ has the following representation:

$$v = a_0 + a_1x_1 + a_2x_2 + a_3x_1x_2 \tag{4.7}$$

for some interpolation constants a_i, $i = 0, \ldots, 3$. Since the degrees of freedom (4.3) vanish over the nonconforming bubble function $x_1x_2 \in \mathcal{Q}^c(K)$, it follows that the restriction of Π to $V_{h,0}^c$ yields [21]

$$\Pi v|_K = a_0 + a_1x_1 + a_2x_2. \tag{4.8}$$

By a scaling argument, one can verify that Π meets (1.5) and therefore the estimates (3.2). Furthermore, for every $v_h \in V_{h,0}^c$ a direct evaluation of the integrals shows (1.3)–(1.4) over rectangular and parallelogram element domains, i.e., the space V_h^{nc} meets (H2).

4.3. The quadrilateral rotated nonconforming element. In [25] Rannacher and Turek introduced two types of quadrilateral nonconforming elements referred to as NR elements. The corresponding local finite element spaces are obtained by rotating the mixed term of the bilinear element, and assuming as local degree of freedom either the average of the function over the edge or its value at the midside node. In this section we consider the nonparametric formulation for rectangular and parallelogram elements with the first choice of degree of freedom. More precisely, for each element $K \in \mathcal{T}$ and with respect to the global coordinate system (x_1, x_2), we set [25]

$$\mathcal{Q}_{\mathcal{R}}^{nc} = \operatorname{span}\{\, 1,\, x_1,\, x_2,\, x_1^2 - x_2^2 \,\} \tag{4.9}$$

and introduce the four degrees of freedom as

$$\mathcal{F}_E(v) = \frac{1}{h_E} \int_E v\, ds \text{ with } E \in \mathcal{E}(K). \tag{4.10}$$

With the corresponding nonconforming finite element space defined as in (4.4) and concordantly $V_{h,0}^{nc}$, it follows that V_h^{nc} meets (H1).

For any $v \in V$, the interpolation operator $\Pi v \in V_{h,0}^{nc}$ is defined as in [25, 21]: For all $E \in \mathcal{E}(K)$ and $K \in \mathcal{T}$,

$$\Pi v \in V_{h,0}^{nc} \quad \text{and} \quad \mathcal{F}_E(\Pi v|_K) = \mathcal{F}_E(v|_K), \tag{4.11}$$

and, hence, as with the Han element, since $\mathcal{F}_E$ vanishes over the nonconforming bubble function $x_1 x_2 \in \mathcal{Q}^c(K)$, the restriction of Π to $V_{h,0}^c \subset V$ is represented locally by (4.8) [21]. Therefore, the above arguments verify (H2).

Remark 2. For the version of the NR element with function evaluation at the midpoints as degree of freedom, (H1) is not satisfied and we refer to section 4.5 for a modification of the NR element.

Remark 3. The proof of Lemma 3.4 for the NR element can be found in [20, 22].

Remark 4. The interpolation operator $\Pi_{\mathcal{P}}$ defined in [2, eqn. (6)] does not, in general, map into the space $X_{\mathcal{P},E}$ of the NR element functions continuous at the midside nodes [2, p. 4]. This results in a gap in the analysis of [2] for this finite element; the remaining assertions in [2] seem to be correct.

Remark 5. The present analysis shows that the augmentation of V_h^{nc} with local bubble trial functions proposed in [23] is not necessary for the error control of $\|\nabla_h e\|$.

Remark 6. The flux $\nabla_h u|_K \cdot \nu_E$ is not required to be constant over each edge E with normal ν_E as in [2]. The latter hypothesis would in fact restrict the analysis to only rectangular meshes.

4.4. The constrained NR element and the P_1-quadrilateral element. The constrained NR finite element (referred to as the CNR element) introduced in [20, 21] is obtained by enforcing a constraint on the degree of freedom of the NR element described in section 4.3. With $\mathcal{Q}_{\mathcal{R}}^{nc}$ denoting here the space of the global trial functions defined over Ω and corresponding to the NR element, the space of the CNR element is then defined as follows:

$$\begin{aligned}\mathcal{Q}_{\mathcal{J}}^{nc} := \Big\{ v \in \mathcal{Q}_{\mathcal{R}}^{nc} : \forall K \in \mathcal{T} \int_{E_1} v\, ds + \int_{E_3} v\, ds = \int_{E_2} v\, ds + \int_{E_4} v\, ds \\ \text{with } E_i, \quad 1 \le i \le 4, \text{ edges of } K \in \mathcal{T} \text{ numbered counterclockwise} \Big\}.\end{aligned} \tag{4.12}$$

For rectangular and parallelogram element domains, considered here, the element is equivalent to the P_1-quadrilateral element of [24]. For homogeneous Dirichlet boundary conditions, it is trivial to check that the space V_h^{nc} meets (H1) for being the CNR space, a subspace of NR. Furthermore, in [20, 21] it is also proved that on the generic element $K \in \mathcal{T}$ with vertices 1, 2, 3, 4 labeled counterclockwise, the interpolation $\Pi v \in V_{h,0}^{nc}$ defined as in (4.11) and for $v \in V_{h,0}^c$ has the representation

$$\Pi v|_K = v_1\phi_1 + v_2\phi_2 + v_3\phi_3 + v_4\phi_4, \tag{4.13}$$

with v_i nodal value of $v \in V_{h,0}^c$ and

$$\begin{aligned}\phi_1(x_1,x_2) &= \frac{1}{4}(1 - x_1 - x_2), \quad \phi_2(x_1,x_2) = \frac{1}{4}(1 - x_1 + x_2), \\ \phi_3(x_1,x_2) &= \frac{1}{4}(1 + x_1 + x_2), \quad \phi_4(x_1,x_2) = \frac{1}{4}(1 - x_1 + x_2)\end{aligned} \tag{4.14}$$

associated with each of such vertices. The arguments of section 4.3 finally show (H2).

4.5. The DSSY element. The main motivation for the definition of this element is to obtain a quadrilateral element with approximation properties similar to those of the Crouzeix–Raviart element. For parallelogram elements these properties were identified in [17] by (i) continuity at the midpoints of each edge, (ii) value of the function at these points as degrees of freedom, and (iii) validity of the orthogonality condition [17, eqn. (6.1)]: For all $v_h \in V_{h,0}^{nc}$ there holds

$$\int_E [v_h]\, ds = 0 \quad \text{ for } E \in \mathcal{E}(\Omega). \tag{4.15}$$

The latter condition plays a crucial role in the proof of optimal error estimates as realized in [17], for instance, by two spaces of local basis obtained by an ad hoc modification of the local basis of the Rannacher–Turek element. Set

$$\theta_\ell(t) = \begin{cases} t^2 - \frac{5}{3}t^4 & \text{for } \ell = 1, \\ t^2 - \frac{25}{6}t^4 + \frac{7}{2}t^6 & \text{for } \ell = 2. \end{cases} \tag{4.16}$$

Then the local space reads

$$\mathcal{Q}_{\mathcal{D}}^{nc} = \operatorname{span}\{1,\, x_1,\, x_2,\, \theta_\ell(x_1) - \theta_\ell(x_2)\} \quad \text{for } \ell = 1, 2, \tag{4.17}$$

and the $\mathcal{Q}_{\mathcal{D}}^{nc}$-unisolvent linear forms read

$$\mathcal{F}_{E_i}(v_h|_K) = v_h|_K(m_{E_i}) \quad \text{ for } E_i \in \mathcal{E}(K),\, 1 \le i \le 4,\, v_h \in \mathcal{Q}_{\mathcal{D}}^{nc}, \tag{4.18}$$

with m_{E_i} midside nodes of the edge E_i. The nonconforming finite element spaces V_h^{nc} and $V_{h,0}^{nc}$ are then defined as in (4.4) with $\mathcal{Q}_{\mathcal{H}}^{nc}$ replaced by $\mathcal{Q}_{\mathcal{D}}^{nc}$. Following [17], one can show that (H1) holds. Furthermore, with the interpolation operator $\Pi : V \mapsto V_{h,0}^{nc}$ defined as in (4.11), one obtains

$$\Pi v \in V_{h,0}^{nc}, \quad \Pi v|_K(m_E) = \frac{1}{h_E}\int_E v\, ds \quad \text{ for each edge } E \in \mathcal{E}(K), \quad K \in \mathcal{T}, \tag{4.19}$$

with the restriction of Π to the space $V_{h,0}^c$ having the local representation (4.8) that implies (H2).

4.6. Hanging nodes. This section discusses 1-irregular meshes and refers to [11] for further details and technicalities. Given an initial regular mesh $\mathcal{T}_0$ of Ω in the sense of Ciarlet [12, 6], a 1-irregular mesh $\mathcal{T}_\ell$ is obtained from $\mathcal{T}_{\ell-1}$ by refining some elements K into four congruent elements by connecting the midside points of the edges of K [4].

Let $\mathcal{N}_H$ denote the set of hanging nodes, $\mathcal{N}_E$ the set of the endpoints of the edges containing one hanging node, $\mathcal{E}_C$ the set of edges with one endpoint in $\mathcal{N}_H$, and $\mathcal{E}_H$ the set of edges containing one hanging node, hereafter referred to as hanging edges. We define the set $\mathcal{N}_R$ of regular nodes as $\mathcal{N}_R = \mathcal{N} \setminus (\mathcal{N}_H \cup \mathcal{N}_E)$ and the set $\mathcal{E}_R$ of regular edges as $\mathcal{E}_R = (\mathcal{E}(\Omega) \setminus \mathcal{E}_C) \cup \mathcal{E}(\Gamma_D)$. It is then possible to construct a partition of unity $(\varphi_z)_{z \in \mathcal{N}_E \cup \mathcal{N}_R}$ on Ω that forms a basis for $V_{h,0}^c$ and define a regularized operator $\mathcal{J} : H^1(\Omega) \mapsto V_h^c$ meeting (2.4)–(2.5) [11].

Under proper constraints for the degrees of freedom for the hanging edges we have the following result that controls the nonconforming part of the error [11]:

$$\min_{\substack{v \in H^1(\Omega) \\ v = u_D \text{ on } \Gamma_D}} \|\nabla_h(u_h - v)\|_{L^2(\Omega)} \le C \left(\sum_{E \in \mathcal{E}_R} h_E \|J_{E,\tau}\|_{L^2(E)}^2 \right)^{1/2} + C\operatorname{osc}(u_D). \tag{4.20}$$

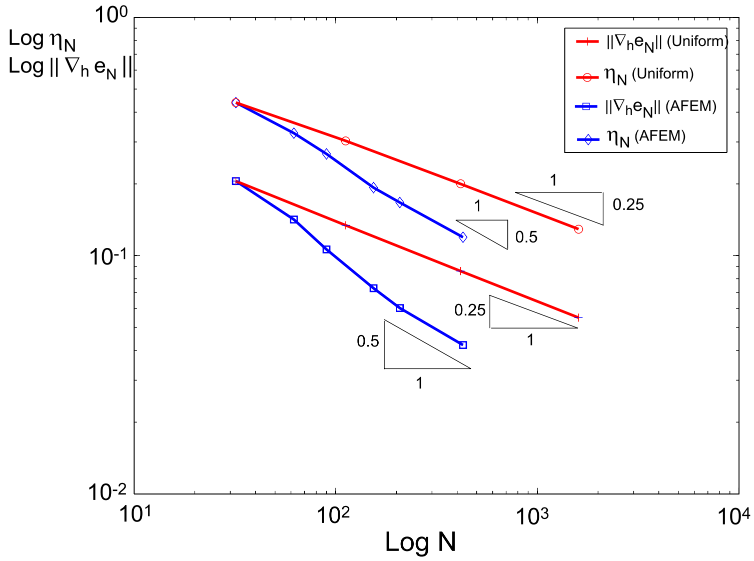

FIG. 2. *Experimental convergence rate of* η_N *and the exact error* $\|\nabla_h e_N\|$ *with respect to the number* N *of degrees of freedom for the adaptive and uniform refinement based on* η_N *and with the NR finite element. The displayed results show* $2.13 \leq \eta_N/\|\nabla_h e_N\| \leq 2.83$ *for adaptive and* $2.13 \leq \eta_N/\|\nabla_h e_N\| \leq 2.35$ *for uniform mesh refinement.*

An integration by parts, use of Young's inequality, the properties of the operator $\mathcal{J}$, and (4.20) finally prove (3.1) with $\eta + \operatorname{osc}(f) + \operatorname{osc}(g) + \operatorname{osc}(u_D)$ and corresponding modifications for the contribution to η from the hanging edges [11].

4.7. Generalizations. If $A \in L^\infty(\Omega; \mathbb{R}^{2\times 2})$ denotes a symmetric positive definite matrix piecewise constant with respect to $\mathcal{T}$, then Theorem 3.1 with corresponding modifications for the definition of η applies also to the elliptic PDE $\operatorname{div} A\nabla u = f$ with boundary conditions $u = u_D$ on Γ_D and $(A\nabla u)\cdot \nu = g$ on Γ_N.

5. Numerical experiment. This section concludes the paper with an example of an adaptive finite element model for the Poisson problem.

5.1. Adaptive finite element method. By rewriting η from (1.6) as $\eta^2 = \sum_{K\in\mathcal{T}} \eta_K^2$, with

$$\eta_K^2 := h_K^2 \|f + \operatorname{div}\nabla u_h\|_{L^2(K)}^2 + \frac{1}{2}\sum_{E\in\mathcal{E}(K)} h_E\big(\|J_{E,\nu}\|_{L^2(E)}^2 + \|J_{E,\tau}\|_{L^2(E)}^2\big),$$

the estimate η and the elemental contributions η_K can be used to generate the triangulations $\{\mathcal{T}_\ell\}_{\ell\in\mathbb{N}}$ in an adaptive way using the following algorithm.

ALGORITHM 1. *Input a coarse mesh* $\mathcal{T}_0$ *with rectangular and/or triangular elements, and set* $\ell = 0$.

(a) *Solve the discrete problem on* $\mathcal{T}_\ell$ *with* N *degrees of freedom.*
(b) *Compute* η_K *for all* $K \in \mathcal{T}_\ell$ *and* $\eta_N := (\sum_{K\in\mathcal{T}} \eta_K^2)^{1/2}$.
(c) *Mark* $K \in \mathcal{M} \subset \mathcal{T}_\ell$ *for refinement into four congruent elements by connecting the midside points of its edges if* $\theta \max_{T\in\mathcal{T}_\ell} \eta_T \leq \eta_K$.
(d) *Mark further elements to ensure at most one hanging node per edge. Define the resulting mesh as the actual mesh* $\mathcal{T}_{\ell+1}$, *update* ℓ, *and go to* (a).

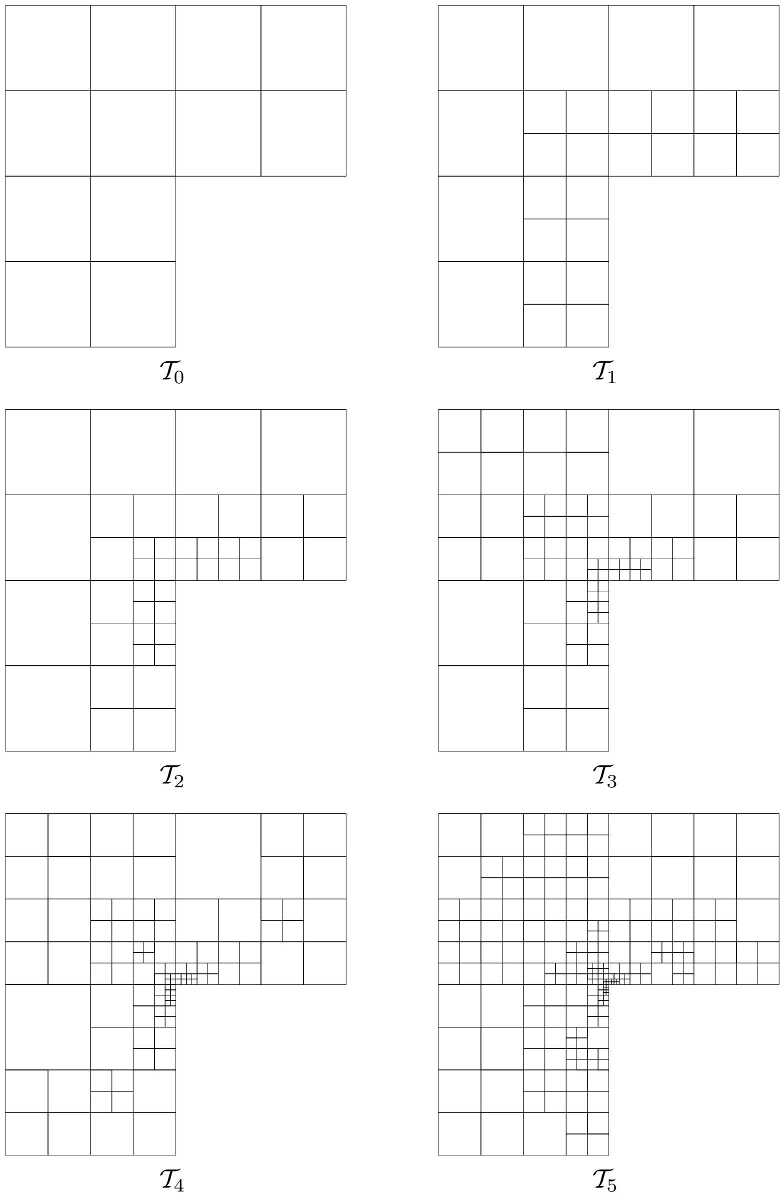

FIG. 3. *Adapted triangulations $\mathcal{T}_0, \ldots, \mathcal{T}_5$ generated with Algorithm* 1 *with $\theta = 1/2$. Notice a local higher refinement towards the reentrant corner.*

The triangulations $\mathcal{T}$ generated by Algorithm 1 are 1-irregular meshes. Error reduction and convergence of the adaptive finite element method based on the bulk criterion has been established in [10] for the Crouzeix–Raviart element.

5.2. Numerical example. On the L-shaped domain $\Omega = [0, 1]^2 \setminus [0.5, 1.0]^2$, we use the NR element defined in section 4.3 to approximate the Poisson problem (1.1) with $f \equiv 0$, $\Gamma_D = \partial\Omega$, $\Gamma_N = \emptyset$, and u_D a smooth function such that in polar coordinates

$$u(r, \theta) = r^{2/3} \sin\left(\frac{2}{3}\theta\right)$$

is the exact solution of (1.1). Figure 2 displays experimental convergence rates for the exact error and the estimate η_N for uniform and adaptive refinement with the corresponding triangulations depicted in Figure 3. The adaptive refinement improves the convergence rate of uniform refinement to the optimal one, $O(N^{-1/2})$, with respect to the number of degrees of freedom, and the convergence rate of the estimate mirrors that of the exact error for both uniform and adaptive refinement.

REFERENCES

[1] M. Ainsworth, *Robust a posteriori error estimation for nonconforming finite element approximation*, SIAM J. Numer. Anal., 42 (2005), pp. 2320–2341.

[2] M. Ainsworth, *A posteriori error estimation for nonconforming quadrilateral finite elements*, Int. J. Numer. Anal. Model., 2 (2005), pp. 1–18.

[3] D. N. Arnold, D. Boffi, and R. S. Falk, *Approximation by quadrilateral finite elements*, Math. Comp., 71 (2002), pp. 909–922.

[4] I. Babuska and A. Miller, *A feedback finite element method with a posteriori error estimation: Part* I. *The finite element method and some basic properties of the a posteriori error estimator*, Comput. Methods Appl. Mech. Engrg., 61 (1987), pp. 1–40.

[5] C. Bernardi and V. Girault, *A local regularization operator for triangular and quadrilateral finite elements*, SIAM J. Numer. Anal., 35 (1998), pp. 1893–1916.

[6] S. C. Brenner and L. R. Scott, *The Mathematical Theory of Finite Element Methods*, 2nd ed., Springer-Verlag, New York, 2002.

[7] C. Carstensen, *Quasi-interpolation and a posteriori error analysis in finite element methods*, M2AN Math. Model. Numer. Anal., 33 (1999), pp. 1187–1202.

[8] C. Carstensen and S. Bartels, *Each averaging technique yields reliable a posteriori error control in FEM on unstructured grids. Part* I: *Low order conforming, nonconforming, and mixed FEM*, Math. Comp., 71 (2002), pp. 945–969.

[9] C. Carstensen, S. Bartels, and S. Jansche, *A posteriori error estimates for nonconforming finite element methods*, Numer. Math., 92 (2002), pp. 233–256.

[10] C. Carstensen and R. H. W. Hoppe, *Convergence analysis of an adaptive nonconforming finite element method*, Numer. Math., 103 (2006), pp. 251–266.

[11] C. Carstensen and J. Hu, *A Priori and A Posteriori Error Estimates for Nonconforming Finite Element Methods with Hanging Nodes*, Preprint, Humboldt-Universität zu Berlin, 2005.

[12] P. G. Ciarlet, *The Finite Element Method for Elliptic Problems*, North–Holland, Amsterdam, 1978; reprinted as Classics Appl. Math. 40, SIAM, Philadelphia, 2002.

[13] P. Clément, *Approximation by finite element functions using local regularization*, RAIRO Anal. Numér., 9 (1975), pp. 77–84.

[14] M. Crouzeix and P.-A. Raviart, *Conforming and nonconforming finite element methods for solving the stationary Stokes equations*, RAIRO Anal. Numér., 7 (1973), pp. 33–76.

[15] E. Dari, R. Duran, and C. Padra, *Error estimators for nonconforming finite element approximations of the Stokes problem*, Math. Comp., 64 (1995), pp. 1017–1033.

[16] E. Dari, R. Duran, C. Padra, and V. Vampa, *A posteriori error estimators for nonconforming finite element methods*, M2AN Math. Model. Numer. Anal., 30 (1996), pp. 385–400.

[17] J. Douglas Jr., J. E. Santos, D. Sheen, and X. Ye, *Nonconforming Galerkin methods based on quadrilateral elements for second order elliptic problems*, M2AN Math. Model. Numer. Anal., 33 (1999), pp. 747–770.

[18] V. Girault and P.-A. Raviart, *Finite Element Methods for Navier–Stokes Equations*, Springer-Verlag, Berlin, 1986.

[19] H.-D. Han, *Nonconforming elements in the mixed finite element method*, J. Comput. Math., 2 (1984), pp. 223–233.

[20] J. Hu, *Quadrilateral Locking Free Elements in Elasticity*, Doctorate Dissertation, Institute of Computational Mathematics, Chinese Academy of Science, 2004 (in Chinese).

[21] J. Hu and Z.-C. Shi, *Constrained nonconforming quadrilateral rotated Q_1-element*, J. Comput. Math., 23 (2005), pp. 561–586.

[22] J. Hu and Z.-C. Shi, *Analysis of Nonconforming-Nonconforming Quadrilateral Rotated Q_1 Element for Reissner–Mindlin Plate*, Preprint 2003–10, Institute of Computational Mathematics, Chinese Academy of Science, 2003.

[23] G. Kanschat and F.-T. Suttmeier, *A posteriori error estimates for nonconforming finite element schemes*, Calcolo, 36 (1999), pp. 129–141.

[24] C. Park and D. Sheen, *$P1$-nonconforming quadrilateral finite element methods for second-order elliptic problems*, SIAM J. Numer. Anal., 41 (2003), pp. 624–640.
[25] R. Rannacher and S. Turek, *Simple nonconforming quadrilateral Stokes element*, Numer. Methods Partial Differential Equations, 8 (1992), pp. 97–111.
[26] L. R. Scott and S. Shang, *Finite element interpolation of nonsmooth functions satisfying boundary conditions*, Math. Comp., 54 (1990), pp. 483–493.
[27] Z.-C. Shi, *The F-E-M test for convergence of nonconforming finite elements*, Math. Comp., 49 (1987), pp. 391–405.
[28] R. Verfürth, *A Review of A Posteriori Error Estimation and Adaptive Mesh-Refinement Techniques*, Wiley–Teubner, Bath, UK, 1996.
[29] E. L. Wilson, R. L. Taylor, W. Doherty, and J. Ghaboussi, *Incompatible displacement models*, in Numerical and Computer Methods in Structural Mechanics, S. J. Fenves, N. Perrone, A. R. Robinson, and W. C. Schnobrich, eds., Academic Press, New York, 1973, pp. 43–57.